JPP Journal of Pharmacy and Pharmacology

JPP 2006, 58: 167–177

Received September 8, 2005
Accepted October 31, 2005
DOI 10.1211/jpp.58.2.0003
ISSN 0022-3573

Design, synthesis and characterization of captopril prodrugs for enhanced percutaneous absorption

Gary P. Moss, Darren R. Gullick, Paul A. Cox, Cameron Alexander, Matthew J. Ingram, John D. Smart and W. John Pugh

Abstract

Most drugs are designed primarily for oral administration, but the activity and stability profiles desirable for this route often make them unsuitable for transdermal delivery. We were therefore interested in designing analogues of captopril, a model drug with poor percutaneous penetration, for which the sustained steady-state blood plasma level associated with transdermal delivery (and which is unattainable orally) would be particularly beneficial. Quantitative structure–permeability relationships (QSPRs) predicted that ester and thiol prodrug derivatives of captopril would have lower maximal transdermal flux (J_m) than the parent drug, since the increases in permeability coefficient (k_p) of prodrugs would be outweighed by the reductions in aqueous solubility. Therefore, the aim of this study was to synthesize a series of prodrugs of captopril and to determine if a QSPR model could be used to design therapeutically viable prodrugs. Molecules with the highest predicted k_p values were synthesized and characterized, and J_m measured in Franz diffusion cells from saturated aqueous donor across porcine skin (fresh and frozen). In-vitro metabolism was also measured. Captopril and the prodrugs crossed the skin relatively freely, with J_m being highest for ethyl to butyl esters. Substantial first-order metabolism of the prodrugs was observed, suggesting that their enhanced percutaneous absorption was complemented by their metabolic performance. The results suggested that QSPR models provided excellent enhancements in drug delivery. This was not seen at higher lipophilicities, suggesting that issues of solubility need to be considered in conjunction with any such use of a QSPR model.

Introduction

The vast majority of drugs are designed for administration via the parenteral or oral routes. Quite often though, their activity and stability profiles make them unsuitable candidates for successful delivery via the transdermal route. This is due to the difficulty in delivering therapeutic quantities of drugs into and across the skin, which is ostensibly due to the barrier nature of the stratum corneum. Absorption across the stratum corneum has been widely reported to be a function of the lipophilicity (as the octanol–water partition coefficient, P) and molecular size of a penetrant. This approach, based on the modelling of the Flynn dataset (Flynn 1990), has been investigated previously by a number of researchers (Potts & Guy 1992, 1995; Cronin et al 1999; Moss & Cronin 2002; Geinoz et al 2004) and reviewed recently (Moss et al 2002). The key equations derived that quantify percutaneous absorption are listed in Table 1. While these models provide excellent mechanistic understandings of percutaneous absorption, they do have substantial limitations. All models are derived from in-vitro experiments using excised human skin, and measurements are made from saturated aqueous solutions. Hence, formulation effects, and to an extent ionization effects are not accounted for by these models, although the latter can be readily accounted for (Lopez et al 1998). Other factors such as the effective therapeutic dose and metabolism of penetrants are not considered in these models.

However, more recently, Magnusson et al (2004) have indicated that, by modelling using the maximal flux (as J_m) and not the permeability coefficient (k_p), molecular weight is the main determinant of percutaneous transport. They indicate that, while previous models describing percutaneous absorption relate k_p to a molecule's physicochemical parameters, J_m is a more relevant parameter as it measures the amount penetrating across the skin, and unlike k_p it does not include an adjustment for the solubility of a molecule. Many strategies

School of Pharmacy, University of Hertfordshire, College Lane, Hatfield, Hertfordshire AL10 9AB, UK

Gary P. Moss

School of Pharmacy & Biomedical Sciences, University of Portsmouth, Portsmouth PO1 2DT, UK

Darren R. Gullick, Paul A. Cox

School of Pharmacy, Boots Science Building, University of Nottingham, University Park, Nottingham NG7 2RD, UK

Cameron Alexander

School of Pharmacy & Biomolecular Sciences, University of Brighton, Lewes Road, Brighton BN2 4GJ, UK

Matthew J. Ingram, John D. Smart

Welsh School of Pharmacy, Cardiff University, Redwood Building, King Edward VII Avenue, Cardiff CF1 3XF, UK

W. John Pugh

Correspondence: G. P. Moss, School of Pharmacy, University of Hertfordshire, College Lane, Hatfield, Hertfordshire AL10 9AB, UK. E-mail: g.p.j.moss@herts.ac.uk

Funding and acknowledgements: The authors would like to thank Ms Wendy Haiko, Bristol-Meyers Squibb, for the provision of captopril. D. R. Gullick is grateful to the School of Pharmacy, University of Portsmouth, for the provision of a research bursary.

Table 1 Algorithms for calculating permeability coefficients across skin and PDMS membranes

a Algorithms for calculating permeability coefficient (k_p), adapted from Flynn (1990).

Range	Low molecular weight (<150 Da)	High molecular weight (>150 Da)
$\log P < 0.5$	$\log k_p = -3$	$\log k_p = -5$
$0.5 \leq \log P \leq 3.0$	$\log k_p = \log P - 3.5$	
$0.5 \leq \log P \leq 3.5$		$\log k_p = \log P - 5.5$
$\log P > 3.0$	$\log k_p = -0.5$	
$\log P > 3.5$		$\log k_p = -1.5$

b Generalized algorithms for predicting permeability and flux across human skin (k_p).

Potts & Guy (1992)	$\log k_p\ (\text{cm h}^{-1}) = 0.71 \log P - 0.0061\ MW - 2.74$
Cronin et al (1999)	$\log k_p\ (\text{cm h}^{-1}) = 0.772 \log P - 0.0103\ MW - 2.33$
Moss & Cronin (2002)	$\log k_p\ (\text{cm h}^{-1}) = 0.74 \log P - 0.0091\ MW - 2.39$
Patel et al (2002)	$\log k_p\ (\text{cm h}^{-1}) = 0.652 \log P - 0.00603\ MW - 0.623\ ABSQon - 0.313\ SsssCH - 2:30$
Magnusson et al (2002)	$\log J_m = -4.52 - 0.0141\ MW$

c Skin permeation models assessed by Wilschut et al (1995).

Brown & Rossi (1989)	$k_p = b1\ (P^{b2}/b3 + P^{b2})$
Fiserova-Bergerova et al (1990)	$k_p = (b1 + b2\ K_{ow})e^{(b3\ MW)}$
McKone & Howd (1992)	$k_p = (b1 + (0.0025/(b2 + b3 + P^{b4})^{-1}(MW^{b5})$
Guy & Potts (1992) (revised, Wilschut et al (1995))	$\log k_p = b1 + b2 \log P + b3\ MW^{0.5}$
Robinson (1993) (revised, Wilschut et al (1995))	$k_p = [(1/K_{pc} + K_{pol}) + (1/K_{aq})]^{-1}$

d Algorithms for predicting permeability across a PDMS membrane.

Cronin et al(1998)	$\log J_m\ (\text{mol cm}^{-2}\ \text{h}^{-1}) = -0.561\ HA - 0.671\ HD - 0.801\ {}^6\chi - 0.383$
Geinoz et al (2002)	$\log k_p = 0.56 \log P - 0.0108\ \Sigma MHBP - 1.16$

Where: kp is the permeability coefficient (cm s^{-1} or cm h^{-1}). b1 to b*n* are regression coefficients for the model equations shown. MW is molecular weight. ABSQon is the sum of absolute charges on oxygen and nitrogen atoms. SsssCH is the sum of E-state indices for all methyl groups. J_m is the maximum flux (mol cm^{-2} h^{-1}). P is the octanol–water partition coefficient. log K_{psc} represents the permeation coefficient of the lipid fraction of stratum corneum: $\log K_{psc} = b1 + b2 \log K_{ow} + b3\ MW^{0.5}$. log K_{pol} permeation coefficient of the protein fraction of the stratum corneum: $\log K_{pol} = b4/MW^{0.5}$. log K_{aq} permeation coefficient of watery (epidermal) layer: $\log K_{aq} = b5W^{0.5}$. HA is the number of hydrogen bond acceptor groups on the molecule. HD is the number of hydrogen bond donor groups on the molecule. ${}^6\chi$ is the 6th order path molecular connectivity. ΣMHBP is the sum of the donor and acceptor potentials of a molecule.

have been employed to enhance the percutaneous absorption of topically applied agents. The use of penetration enhancers, supersaturated solutions and iontophoresis have all been widely researched and reviewed (Barry 1983; Bronaugh & Maibach 1999; Kalia et al 2004; Leboulanger et al 2004; Valenta & Auner 2004).

Significant research has been conducted in the percutaneous penetration of prodrugs. Udata et al (1999) synthesized four propranolol ester prodrugs, and investigated the influence of stereochemistry on skin permeability and metabolism. They concluded that increasing the lipophilicity of their prodrugs increased permeability significantly. Similar findings have been found by other researchers, who have investigated the permeation of prodrugs of naltrexone (Stinchcomb et al 2002), carbamazepine (Fourie et al 2004) and ketorolac (Doh et al 2003).

We are interested in designing analogues of currently-used drugs for which the sustained steady-state blood plasma level associated with transdermal delivery (and which is usually unattainable orally) would be of particular clinical benefit. The captopril prodrugs (Figure 1) are based on chemical bonds that are readily metabolized to the original, therapeutically active molecule. Captopril (Figure 1) is an angiotensin converter enzyme (ACE) inhibitor and would potentially benefit from the zero-order controlled release achieved by transdermal drug delivery, minimizing or avoiding the 'peaks and troughs' classically associated with oral dosing. Further, captopril is a relatively hydrophilic molecule with a reported log P_{exp} of 0.34 (Ranadive et al 1992) and as such is not readily amenable to percutaneous transport.

Therefore, the aim of this study was to design a series of prodrugs based on captopril that would offer enhanced percutaneous absorption compared with the parent drug, and which would be rapidly metabolized back to the parent molecule once absorbed. Quantitative structure–permeability relationships (QSPRs) were used to select candidate prodrugs, and lead candidates would be synthesized and characterized. Their in-vitro transport across PDMS (Silastic) membranes and porcine skin was measured. In particular, we were interested in assessing the applicability of QSPR models (the 'Potts and Guy'-type models (Potts & Guy 1992, 1995; Moss & Cronin 2002) and those proposed by Magnusson et al (2004)) to the development

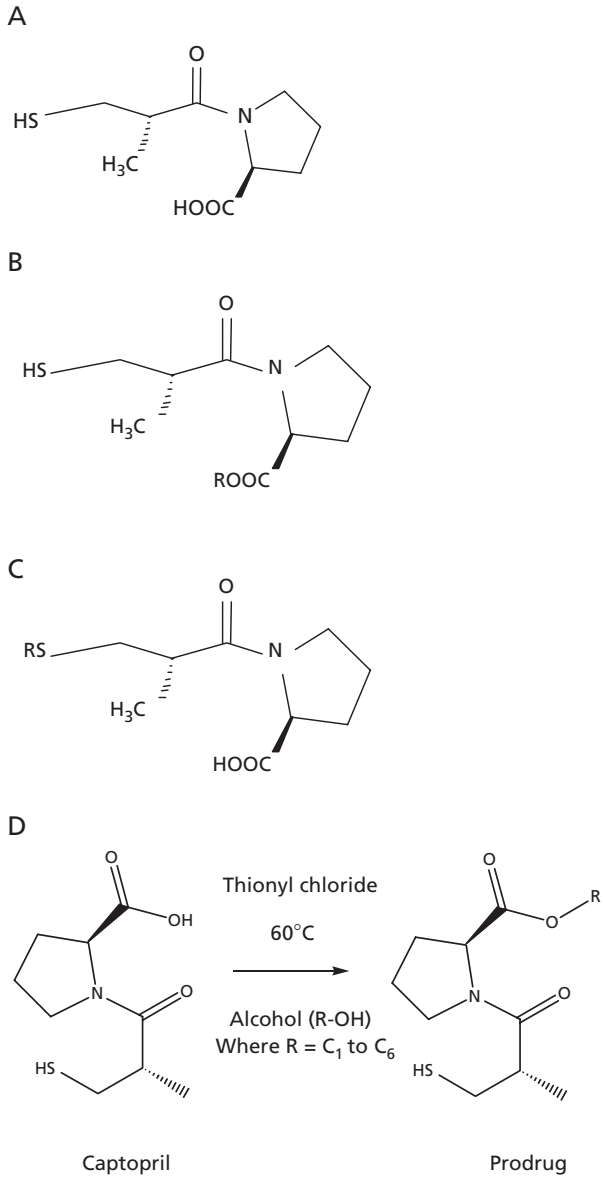

Figure 1 The chemical structures of (A) captopril and the generic structures of the (B) carboxyl ester and (C) thiol ether captopril prodrugs, where R = an n-alkyl chain of length C_1–C_6. Part D shows the reaction scheme for the synthesis of captopril ester prodrugs.

of prodrug candidates that offer enhanced drug delivery compared with their parent compounds.

Materials and Methods

Materials and instrumentation

Captopril was a gift from Bristol-Meyers Squibb PRI (Wallingford, CT, USA). All alcohols for synthesis and methanol for the chromatographic analysis (all HPLC grade), HPLC-grade water, sodium dihydrogen orthophosphate, disodium hydrogen orthophosphate, sodium chloride, thionyl chloride, iodine, high-vacuum grease, Parafilm, disposable syringes and quartz UV cuvettes were obtained from Fisher Scientific, UK. TLC plates (60GF on aluminium) were obtained from Aldrich Chemical Co., UK. Porcine liver esterases were obtained from Sigma Chemical Co., UK. Silastic membranes were supplied by Dow Corning Ltd. (Abingdon, UK). Cyanoacrylate glue was obtained from Niceday Ltd, UK. Pig skin (from pig ears) was obtained as a waste product of food use from a local supplier. It was prepared for use as described by Taylor et al (2002). Sample vials used in LC analysis were obtained from Agilent Ltd, UK. Syringe filters (0.2 μm) were obtained from Chromacol Ltd, UK. Analysis and characterization were carried out using Franz-type diffusion cells (10-mm aperture, 3 cm^3 receptor compartment volume) D & J Jones, Loughborough, UK), Helios B UV spectrophotometer (Helios Ltd, UK), Research Series FT-IR (Mattson Instruments Inc., UK), Jeol JNM-LA400 400MHz NMR (Jeol Ltd, UK), FT-Raman spectrometer (model NXR 9610, Nicolet, UK), Agilent 1100 electrospray LC-MS (Agilent Ltd, UK), Hewlett Packard HP5890 GC-MS with BPX-5 capillary column (Hewlett Packard Inc., UK) and a digital polarimeter (AA-5 Series, Optical Activity Ltd, UK).

Selection of molecules

It was proposed to modify captopril by considering the formation of carboxyl esters, thiol ethers and dimers (Figure 1). Prodrugs to be synthesized were chosen by estimation of their predicted k_p values, based on the quantitative structure–permeability relationship by Moss & Cronin (2002), and are listed in Table 1. Using SMILES (Simplified Molecular In-Line Entry System) codes, log P and solubility were calculated from the IA program (http://www.logp.com/) and the EPI (Estimations Programme Interface) Suite software (Version 3.12, Syracuse Research Corporation), and Virtual Computational Chemistry Laboratory (VCCL: http://146.107.217.178/). Melting points were estimated by the EPI Suite software. Predicted log P values that were closest to experimentally determined values (Ranadive et al 1992) were preferentially used. Those molecules, or series of molecules, which exhibited the highest theoretical fluxes were selected for synthesis and in-vitro absorption studies.

Synthesis

The prodrugs were synthesized by a modification of a previously published method (Tai et al 1995). Captopril (5 mmol, 1.09 g) was dissolved in the appropriate alcohol (C_1–C_6, 25 mL). Thionyl chloride (0.1 mL, 1.35 mmol) was then added dropwise at 0 °C. The reaction mixture was heated at 60 °C for 4 h. The excess alcohol and thionyl chloride produced hydrogen chloride gas, and was removed in-vacuo to yield the ester. All prodrugs were characterized by ^1H and ^{13}C NMR, FT-IR, and Raman spectroscopy (the latter of which was used to confirm the absence of S-S bonds which are characteristic of captopril degradation and are not readily observed by IR spectroscopy), GC-MS and determination of their optical rotation. Aqueous solubility of all prodrugs was determined by the method reported by Lebosse et al (1996). Briefly, excess amount of the solute was stirred for 24 h in

Table 2 Permeability coefficients and flux (as appropriate) predicted by QSPR equations, and log P, melting points and solubility predicted by software packages

Molecule	In-vitro Metabolism		P^1	Molecular weight	Aqueous solubility (mM)		k_p (cm h^{-1} $\times 10^{-4}$)	J_m (μmol cm^{-2} h^{-1})					
	k(h^{-1})	Half-life (h)	Calc.		Calc.[2]	Exp.	Predicted	Predicted			Experimental porcine		Experimental silastic
							Human	Human		Silastic	Fresh ± s.e.	Frozen ± s.e.	± s.e.
							Moss[3]	Moss[4]	Magnusson[5]	Cronin[6]			
Captopril	*	*	4.23	217.29	77.2	66.7	1.25	0.0096	0.0094	13.5	0.0198 ± 0.0027	0.0980 ± 0.0031	0.2630 ± 0.0409
Methyl ester	0.044	15.750	15.1	231.29	22.1	38.7	2.39	0.0053	0.0051	43.5	0.0494 ± 0.0089	0.1392 ± 0.0728	0.1890 ± 0.0334
Ethyl ester	0.098	7.100	45.6	245.29	8.84	35.6	4.03	0.0036	0.0027	34.4	0.7841 ± 0.2177	0.2906 ± 0.0654	0.3510 ± 0.0334
Propyl ester	0.082	8.470	140	259.29	3.54	18.3	6.89	0.0024	0.0015	29.1	0.2885 ± 0.0447	0.2237 ± 0.0427	0.4054 ± 0.0000
Butyl ester	0.031	22.345	461	273.29	1.33	18.0	12.4	0.0017	0.0008	20.8	0.2619 ± 0.0878	0.1942 ± 0.0587	0.7400 ± 0.0883
Pentyl ester	*	*	1630	287.29	0.48	8.00	23.5	0.0011	0.0004	19.5	0.0551 ± 0.0042	0.0086 ± 0.0019	0.5400 ± 0.0334
Hexyl ester	*	*	4730	301.29	0.17	2.29	38.6	0.0007	0.0002	16.3	0.0000 ± 0.0000	0.0028 ± 0.0008	0.2460 ± 0.0883
Methyl thiol	*	*	5.16	231.31	50.7	*	1.08	0.0055	0.0051	15.2	*	*	*
Ethyl thiol	*	*	18.1	245.34	16.4	*	2.03	0.0033	0.0027	11.5	*	*	*
Propyl thiol	*	*	31.1	259.37	6.21	*	2.26	0.0014	0.0015	8.4	*	*	*
Butyl thiol	*	*	85.4	273.39	2.04	*	3.56	0.0007	0.0008	7.8	*	*	*
Pentyl thiol	*	*	306	287.42	0.69	*	6.83	0.0005	0.0004	6.6	*	*	*
Hexyl thiol	*	*	994	301.45	0.24	*	12.2	0.0003	0.0002	5.6	*	*	*

[1]From mean logP value calculated by AlogPs, IA logP, CLOGP, miLogP, KOWWIN, XLOGP (Virtual Computational Chemistry Laboratory, http://146.107.217.178/) and from the EPI Suite Software (v. 3.12) and IAP software (http://www.logp.com). [2]From mean logS value calculated by ALOGpS IA logS (Virtual Computational Chemistry Laboratory, http://146.107.217.178/) and fragment prediction method in the EPI Suite Software (v. 3.12). [3]From the equation of Moss & Cronin (2002) (Table 1). [4]From product of calculated aqueous solubility and k_p. [5]Magnusson et al (2004) (Table 1). [6]Cronin et al (1998) (Table 1). [7]For J_m experimental results, n = 6.

deionized water. The solutions were then filtered (using a 0.2-μm PTFE filter paper with polypropylene housing) and then ultra-centrifuged at 30000 rev min^{-1} for 1 h. The supernatant was collected and assayed by potentiometric titration as per the British Pharmacopoeial method for captopril, using 0.005 M iodine (British Pharmacopoeia 2003). Prepared saturated solutions were stored at 0°C and used within 48 h. All solutions were checked for degradation before use in diffusion experiments. Characterization of the prodrugs was as follows.

Captopril methyl ester

^{1}H NMR δ/ppm (400 MHz, $CDCl_3$): 1.2 (d, 3H, CH_3 side chain); 1.8 (t, 1H, SH), 2.0 (complex m, 2H, CH_2 ring); 2.25 (m, 2H, CH_2 ring); 2.50 (complex m, 1H, CH); 2.7 (t, 2H, aliphatic CH_2); 3.6 (m, 2H N-CH_2 ring); 4.4 (dd, 1H, COCH ring); 4.8 (s,3H ester CH_3).

^{13}C NMR (100.54 MHz, $CDCl_3$): δ=17.05 (CH_3 side chain), 24.81 (CH_2 ring), 27.54 (CH_2-SH), 29.08 (CH_2 ring), 42.52 (C(CH_3)CO side chain), 47.01 (N-CH_2 ring), 52.16 (CH_3 ester), 58.63 (COCH ring), 172.68 (CO ester), 173.68 (CO amide).

IR (cm^{-1}, thin film on NaCl plates): C-H Str. 2958 to 2873, C-S Str. 2360, C=O Str. 1734, C=O Str. 1652, C-H bend 1457 to 1435, C-N str. 1368 to 1048.

Optical rotation α^D −143.3° at 20.3°C in methanol.

GC-MS method: injection port temperature 250°C, MS temperature 280°C, oven program: 60°C 3 min, ramp at 20°C min^{-1} to 250°C, hold at 250°C for 8 min. Methyl ester in DCM gave a single peak at 11.06 min, the molecular weight of MH^+ by mass spectrum was 231.

Captopril ethyl ester characterization features as methyl ester, with differences listed as follows

^{1}H NMR δ/ppm (400 MHz, $CDCl_3$): 1.2 (complex m, 3H, ester CH_3 moved from 4.8); 4.1 (dd, 2H, CH_2 side chain).

^{13}C NMR (100.54 MHz, $CDCl_3$): δ=14.13 (CH_3 ester), 61.02 (CH_2 side chain).

Optical rotation α^D −140.1° at 20.3°C in methanol.

GC-MS: ethyl ester in DCM gave a single peak at 13.03 min, the molecular weight of MH^+ by mass spectrum was 245.

Captopril propyl ester characterization features as methyl ester, with differences listed as follows

^{1}H NMR δ/ppm (400 MHz, $CDCl_3$): 0.9 (t, 3H, ester CH_3 moved from 4.8); 1.6 (m, 2H, CH_2 side chain); 4.1 (dd, 2H, CH_2 side chain).

^{13}C NMR (100.54 MHz, $CDCl_3$): δ=10.37 (CH_3 ester), 21.96 (CH_2 side chain), 66.59 (CH_2 side chain).

Optical rotation α^D −142.5° at 20.3°C in methanol.

GC-MS: propyl ester in DCM gave a single peak at 13.51 min, the molecular weight of MH^+ by mass spectrum was 259.

Captopril butyl ester characterization features as methyl ester, with differences listed as follows

^{1}H NMR δ/ppm (400 MHz, $CDCl_3$): 0.9 (t, 3H ester CH_3 moved from 4.8); 1.3 (m, 2H, CH_2 side chain); 1.6 (t, 2H, CH_2 side chain); 4.1 (m, 2H, CH_2 side chain).

^{13}C NMR (100.54 MHz, $CDCl_3$): δ=13.69 (CH_3 ester), 19.05 (CH_2 side chain), 30.59 (CH_2 side chain), 64.88 (CH_2 side chain).

Optical rotation α^D −133.8° at 20.3°C in methanol.

GC-MS: butyl ester in DCM gave a single peak at 14.21 min, the molecular weight of MH^+ by mass spectrum was 273.

Captopril pentyl ester characterization features as methyl ester, with differences listed as follows

^{1}H NMR δ/ppm (400 MHz, $CDCl_3$): 0.9 (t, 3H ester CH_3 moved from 4.8); 1.3 (m, 4H, CH_2 side chain); 1.6 (m, 2H, CH_2 side chain); 4.1 (dd, 2H, CH_2 side chain).

^{13}C NMR (100.54 MHz, $CDCl_3$): δ=13.95 (CH_3 ester), 24.80 (CH_2 side chain), 28.52 (CH_2 side chain), 30.59 (CH_2 side chain), 64.88 (CH_2 side chain).

Optical rotation α^D −143.7° at 20.0°C in methanol.

GC-MS: pentyl ester in DCM gave a single peak at 14.99 min, the molecular weight of MH^+ by mass spectrum was 287.

Captopril hexyl ester characterization features as methyl ester, with differences listed as follows

^{1}H NMR δ/ppm (400 MHz, $CDCl_3$): 0.9 (t, 3H ester CH_3 moved from 4.8); 1.3 (m, 6H, CH_2 side chain); 1.6 (m, 2H, CH_2 side chain); 4.1 (dd, 2H, CH_2 side chain).

^{13}C NMR (100.54 MHz, $CDCl_3$): δ=13.95 (CH_3 ester), 24.80 (CH_2 side chain), 28.52 (CH_2 side chain), 30.59 (CH_2 side chain), 37.33 (CH_2 side chain), 64.88 (CH_2 side chain).

Optical rotation α^D −148.9° at 20.3°C in methanol.

GC-MS: hexyl ester in DCM gave a single peak at 15.87 min, the molecular weight of MH^+ by mass spectrum was 301.

In-vitro diffusion studies

Franz cell studies were based on methods reported previously (Woolfson et al 1998; Taylor et al 2002). Static diffusion cells were employed, along with a protocol employing periodic removal and replacement of the receptor compartment. Receptor compartments were filled with phosphate buffered saline (pH 7.4). Ensuring that no bubbles were present, the membrane was placed across the top of the receptor chamber. Membranes were secured in place with a cyanoacrylate adhesive. Side arms were sealed with glass caps lubricated with vacuum grease. All cells were held together with spring-loaded clamps. Saturated aqueous solutions of captopril or its prodrugs (1.0 mL) were introduced to the donor compartment of each cell, and the donor compartment was then occluded with Parafilm. The cells were then placed in a water bath at 37°C. The cell was dismantled and the receptor phase removed for analysis periodically (to avoid the possibility of bubbles being introduced via the sidearm of the cell) during a 24-h period (e.g. after 1, 2, 3, 4, 6, 8, 16 and 24 h).

For diffusion experiments employing a Silastic membrane, UV analysis was employed at λ_{max} 206 nm. A calibration graph was linear in the range 0.00012–0.00968% w/v for all molecules. LC was employed (ODS column with a mobile phase of 50:50 methanol:water, and typical run times between 10 and 30 min) to analyse all samples where fresh or frozen porcine skin was used as the diffusing membrane. Local approval was obtained for the use of porcine skin as a

residue of food use. To ensure adequate comparisons could be made between fresh and frozen skin, samples were taken from the same site of an animal; half of the tissue was frozen as described by Taylor et al (2002) and the other half was used fresh. Analysis was by diode array detection (calibration range linear in the range 0.002–0.2% w/v) and MS was employed to confirm the structural identity of analytes. Where appropriate, the use of diode-array LC-MS allowed a simultaneous identification and quantification of captopril and its prodrug. Drug concentrations quoted were the combined concentrations of the prodrug and any captopril observed, if applicable.

As a quality check, before all Franz cell diffusion experiments, the prodrug to be used was sampled and analysed by GC-MS (for neat oils of prodrugs) and LC-MS (for saturated aqueous solutions). No degradation, either at room temperature or at −78°C, was observed.

In-vitro metabolism

Prodrug metabolism was assessed in-vitro by a variation of a method reported by Ostacolo et al (2004). Each ester (400 μg, 1000 μL, n = 4) was added to phosphate buffered saline (8720 μL) and equilibrated at 37°C for 45 min, before adding porcine liver esterase (50 U, 28 μL of a suspension in ammonium sulphate). Blank samples without esterase were run for each prodrug. Samples (0.5 mL) were taken after 0.5, 1.0, 1.5, 2.0, 3.0, 4.0, 5.0 and 24 h. The samples were immediately shaken with 1 mL acetone, to precipitate the esterase and to stop any further metabolism. Samples were filtered through 0.2-μm Teflon filters and analysed by the HPLC method described above.

Results and Discussion

Synthesis and characterization of prodrugs

Estimated values of k_p, calculated from QSPR equations, are shown in Table 2, and suggest that ester prodrugs should be more successful as potential transdermal drug candidates than the thiols. The n-methyl to n-hexyl carboxyl esters were therefore synthesized as described above. The experimental conditions for ibuprofen prodrugs (Tai et al 1995) resulted in the formation of diastereoisomers of captopril, as confirmed by NMR, optical rotation measurements, and the presence of two distinct peaks in GC analysis. Lowering of temperature and reaction time yielded captopril esters with retention of the original stereochemistry and was confirmed by NMR, FT-IR, GC-MS, Raman spectroscopy (which confirmed retention of the −SH peak at 2576 nm and absence of the disulphide peaks between 430 and 550 nm that were characteristic of captopril dimerization) and optical rotation.

Gaseous residues and excess alcohols were removed in-vacuo. Yields were high (>98% in all cases). All the prodrugs produced were oils at room temperature. This was substantially different from the melting points of 102–137°C predicted by the various software packages (discussed previously in the Materials and Methods section). Table 2 shows that the predicted and the experimental aqueous solubility varied by factors up to 40. These discrepancies may have partly accounted for the differences between predicted and experimental rankings of J_m for the prodrugs.

Molecular modelling, membrane transport and percutaneous absorption

One of the issues in this study was the use of porcine skin rather than human tissue. Porcine skin has been used widely as a model for human skin, and many researchers have indicated that it is the animal skin which bears the closest resemblance to human skin (Wester & Noonan 1980). More specifically, Wu et al (1997) examined the percutaneous absorption of captopril across human, pig, rabbit, rat and mouse skin. They found that permeation across human skin was similar to pig skin, and that rabbit, rat and mouse skin all significantly over-estimated percutaneous absorption. The results presented in this study should therefore be interpreted with this potential limitation in mind.

We were concerned about the possible degradation of the prodrugs before their use for in-vitro experiments. Therefore, samples for analysis were normally prepared (i.e. synthesized and purified) immediately before the Franz cell experiment was run. However, it was necessary on a few occasions to prepare the prodrug several days in advance, and store it at −78°C. As a quality assurance check, before and after all Franz cell experiments, the donor phase solutions or neat prodrugs were sampled and analysed by GC-MS or LC-MS, as appropriate. No degradation, either at room temperature or at −78°C, was observed. Further, non-enzymatic hydrolysis was not observed in any diffusion experiments. This might call into question the viability of freshly prepared and mounted porcine skin, particularly in the absence of a suitable medium (e.g. glucose) to keep the tissue viable, and metabolically active. However, in all cases fresh skin was used the same day as it was harvested, usually within hours of becoming available, and it was unlikely that all metabolic activity would have ceased so rapidly. Typically, skin can remain viable for up to 12 h after cultivation but requires a modified receptor phase to preserve viability after this time (Collier et al 1989). However, measuring in-situ metabolism via Franz cells was not the aim of the diffusion studies; rather, we were concerned about the stability of the prodrugs added to the donor phase and in determining permeation into a widely used receptor phase, ostensibly to allow us to model these results more widely in future studies. Separate in-vitro metabolism experiments are discussed below.

Martinez et al (2001) discussed a case study which highlighted skin sensitivity to topical captopril in a single patient. It is difficult to predict the sensitizing of captopril esters unless a robust dataset exists for the range of molecules of interest. In this study, captopril was essentially chosen as a 'proof of concept' molecule, thus a less sensitizing ACE-inhibitor might be chosen at a later stage of this research.

Table 1 shows that, while there was a wide range of generalized and in some cases very specific QSPR models available for the prediction of percutaneous absorption, they may be mostly categorised as variations and iterations of the Potts and Guy equation (Potts & Guy 1992):

$\log k_p\ (cm\,h^{-1}) = 0.71 \log P - 0.0061\,MW - 2.74$
$(n = 93;\ r^2 = 0.67;$ s not reported; F not reported)

The main determinants were an intermolecular binding term (usually expressed by log P as 'lipophilicity') and size. Whilst they are at present restricted to simple aqueous solutions of un-ionized permeants (Moss et al 2002) they should successfully rank maximal flux for captopril and its prodrugs. J_m rankings were therefore assessed in two ways. The equation of Magnusson et al (2004) predicts J_m simply from molecular weight:

$\log J_m = -4.52 - 0.0141\,MW$
$(n = 278;\ r^2 = 0.688;\ P < 0.001)$

The other equations in Table 2 enabled prediction of k_p. J_m could then be estimated from the product of k_p and aqueous solubility, calculable by a range of algorithms, or measured experimentally. We used the equation of Moss & Cronin (2002) as it was the most recent example of a QSPR model using log P and molecular weight, and could be applied without the need for specific molecular modelling software.

$\log k_p\ (cm\,h^{-1}) = 0.74 \log P - 0.0091\,MW - 2.39$
$(n = 116;\ s = 0.42;\ R_{adj}{}^2 = 0.82;$ RCV2 = 0.81; F = 266; and *t*-values: log *P* 22.8; MW, −16.6; $P < 0.0001$ for both variables)

These models should be applied with significant caveats. For example, Flynn (1990) listed different models for different log P ranges (Table 1). Cut-off points were defined at log P values of 3.0 and 3.5. Wilschut et al (1995) indicated that separate models should be used for high and low log P values. Therefore, while the use of QSPR models provided an excellent predictor of permeability, it was limited by the range of data in the model itself (i.e. the range of physicochemical parameters, such as log P, of the molecules in the dataset). Further, the application of a linear statistical analysis to skin absorption may not be compatible with the non-linear response observed for the penetration of very lipophilic molecules. It has been reported (Taylor et al 2002) that very lipophilic molecules (log $P > 3.0$) do not penetrate skin in substantial amounts so that their prediction is greatly overestimated by linear QSPR models.

The results of the diffusion cell experiments are summarised in Table 2. Conventional plots of drug release over time show a sigmoid profile typical of in-vitro drug diffusion. One key issue in this study was the lack of correlation observed between diffusion experiments using PDMS (Silastic) membranes and porcine skin (Figures 2 and 3). Six replicates were performed for Franz cell experiments with fresh and frozen skin, and three for Silastic. Mean flux values for captopril and the prodrugs were therefore calculated for each membrane, and these analysed by two-way analysis of variance using chain length of prodrug and membrane as factors. A *P* value of 0.037 indicated differences amongst the membranes. Inspection of the 95% confidence interval plots showed that those for the Silastic mean flux ($0.386\ \mu mol\,cm^{-2}\,h^{-1}$) and frozen skin ($0.100\ \mu mol\,cm^{-2}\,h^{-1}$) did not overlap, suggesting that flux was significantly greater ($P < 0.05$) from Silastic than from frozen skin. Regression analysis determined that comparisons of $J_{Silastic}$ against $J_{Fresh\ Skin}$ and $J_{Frozen\ Skin}$ gave correlations no greater than $r^2 = 0.03$. Good correlations existed between fresh and frozen skin experiments ($r^2 = 0.71$). Silastic and similar materials have been widely used and accepted as being able to mimic transport across skin, and have found widespread use as a rapid and labour-saving alternative to animal or human skin, particularly in preliminary studies. While Silastic has also been shown to over-estimate transport when compared with human or porcine skin (Woolfson et al 1992, 1998), its permeability to

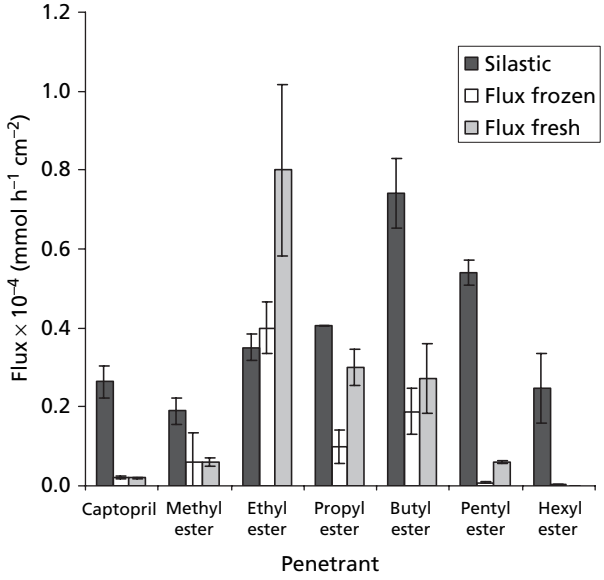

Figure 2 A comparison of flux (J_{max}) across Silastic and fresh and frozen porcine skin for captopril and its carboxyl ester prodrugs.

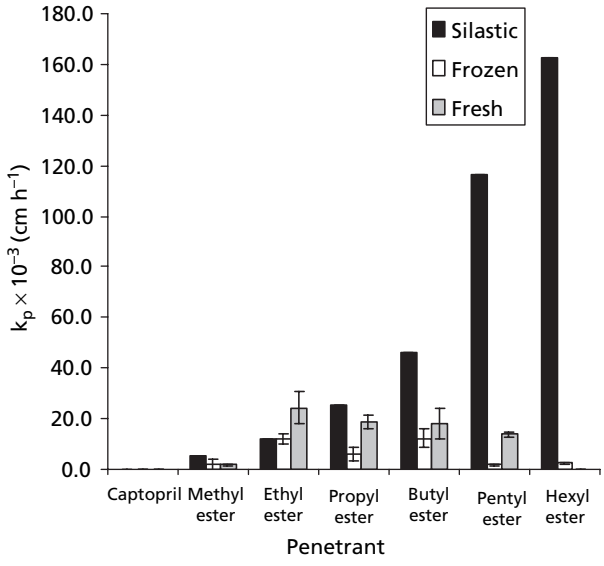

Figure 3 A comparison of the permeability coefficient (k_p) across Silastic and fresh and frozen porcine skin for captopril and its carboxyl ester prodrugs.

exogenous chemicals usually correlates well to these membranes, despite being a homogenous membrane. Previously, Cronin et al (1998) derived a QSPR for predicting the flux of molecules across Silastic membranes:

$$\log J_m = -0.561\ HA - 0.671\ HD - 0.801\ {}^6\chi - 0.383$$
$$(n = 242; s = 0.46; r = 0.90; F = 338)$$

This indicated that the only significant descriptors governing flux across PDMS membranes were molecular size and hydrogen bonding (Table 1). A direct comparison between QSPR models for skin and PDMS is inappropriate given that they predict k_p and flux, respectively, and employ substantially different datasets. However, it was clear that by qualitatively comparing the models there were substantial differences which were reflected in the experimental results presented in this study.

Therefore, the suitability of PDMS membranes to act as substitute for skin was clearly questionable in this study. This was most likely due to the large lipophilicity range of the prodrugs examined in this study (Table 1). The stratum corneum contains both lipophilic and hydrophilic domains, and lies above the viable epidermis as the outermost layer of the skin. It provides the main barrier to the percutaneous absorption of exogenous chemicals, and a molecule must possess a degree of lipophilicity to partition into the stratum corneum. However, it must also possess hydrophilic properties so that it can partition between the stratum corneum and the underlying viable tissues, which are increasingly hydrophilic in nature. A PDMS membrane does not replicate this complexity and is amenable to the diffusion of increasingly lipophilic molecules. Hence, it may be appropriate to consider that Silastic is limited in reflecting the barrier properties of porcine or human skin within certain ranges of log P. Clearly, the nature of the receptor phase may also be an issue in such in-vitro experiments. An aqueous receptor phase will limit the solubility of lipophilic materials. However, the use of the permeability coefficient (k_p) and not flux should correct for any disparities in solubility, particularly over the range of log P investigated in this study. However, the use of non-aqueous materials (i.e. ethanol, bovine serum albumin, surfactants) would not enhance the receptor phase solubility of all prodrugs equally and these were not used in this study.

Maximal flux values, predicted by the methods of Magnusson et al (2004) and Moss & Cronin (2002), are plotted in Figure 4, along with the experimental values for captopril and its prodrugs through fresh and frozen pig skin. Due to issues of scaling, the data has been divided into two plots, with Figure 4A showing the flux data through fresh porcine skin, and Figure 4B showing the rest of the results. Two-way analysis of variance of flux (n = 6), using prodrug chain length and membrane as factors, showed that flux across fresh skin (mean 0.207 μmol cm^{-2} h^{-1}) was greater than for frozen (0.100 μmol cm^{-2} h^{-1}) ($P = 0.007$). Significant differences ($P < 0.001$) existed amongst the prodrugs, and inspection of the 95% confidence interval plots showed that the ethyl ester mean (0.521 μmol cm^{-2} h^{-1}) was significantly higher than all others. Both mathematical methods predictions were unsuccessful in predicting the increased flux of the esters over the parent captopril. The predictions were not improved if experimental aqueous solubility values were used instead of the predicted ones ($r^2 < 0.03$ in all cases). The Silastic model (not shown for clarity) predicted an increase peaking for the lower chain length esters. The skin experiments showed that flux peaked for the ethyl ester, suggesting that experimental results using simple membrane models would give a better indication of the feasibility of prodrug design than would molecular modelling. The extent of the inaccuracy of the mathematical modelling can be assessed by Figure 5A, which compared the flux though frozen skin with the mean values from mathematical modelling. While it must be acknowledged that the high values may not be applicable to human

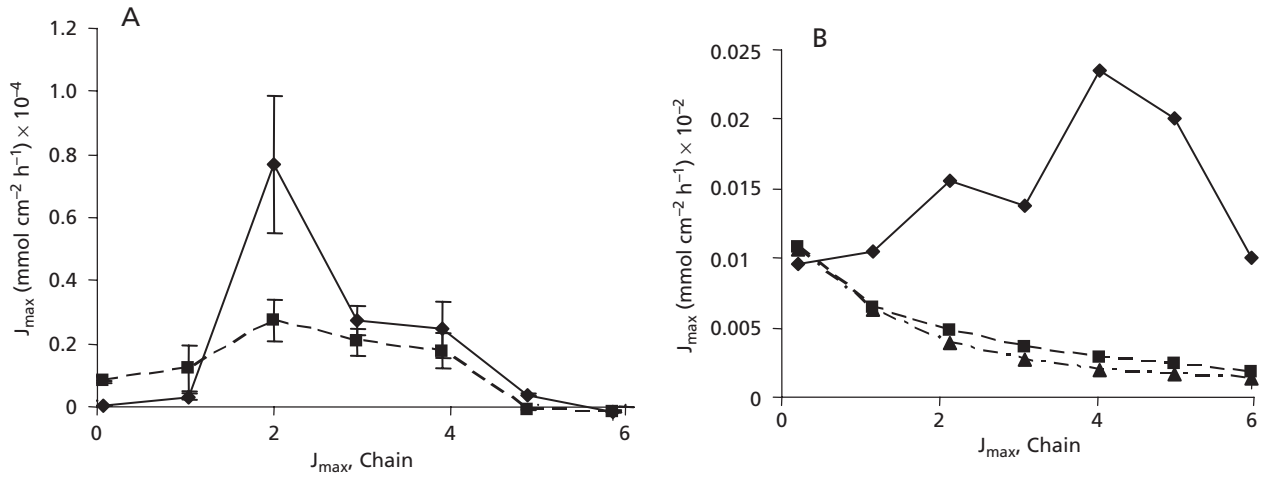

Figure 4 Maximal flux values, for captopril and its prodrugs though fresh and frozen pig skin. A. J_{max} for transport across fresh (◆) and frozen (■) pig skin. B. J_{max} predicted by the methods of Magnusson et al (2004) (▲) and Moss & Cronin (2002) using the predicted (■)) and the measured (◆) solubility. Note: error bars are not shown in B, as the data presented were modelled (predicted) results. A. Experimental data was based on n = 6 for skin experiments and n = 3 for Silastic experiments. Please note the different scales used in A and B.

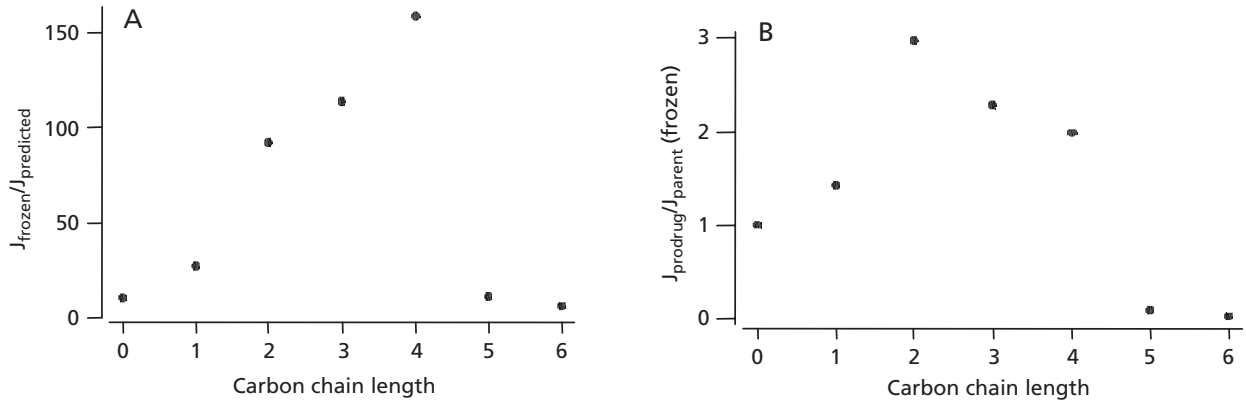

Figure 5 Comparisons of the flux though (A) frozen skin with the mean values from mathematical modelling and (B) across frozen pig skin between the parent molecule and prodrug. Note: error bars do not appear on these graphs as they are comparisons where experimental results were related to predicted results. In all cases, experimental data was based on n = 6 for skin experiments and n = 3 for Silastic experiments.

skin, it was apparent that J_m for the prodrug was greatly underestimated. Frozen skin results (Figure 5B) suggested that the ethyl ester should have a maximal flux approximately three times higher than the captopril parent. The mechanism for this, admittedly modest, increase in percutaneous transport was unclear. We hypothesized that the greater lipophilicity of the prodrugs produced a higher concentration in the outermost layer of the stratum corneum. Enzymatic cleavage might therefore produce a localized supersaturation of captopril which would enhance captopril flux. This was unlikely as no parent drug was found in the receptor phase.

In summary, QSPRs suggested that esters and thiol derivatives of captopril would have lower J_m values than the parent, with J_m decreasing with ester chain length. In practice the esters had flux values up to 0.8 μmol cm^{-2} h^{-1} for the ethyl ester (≈100 times that predicted), peaking for the intermediate chain lengths. These large differences could not be explained by the higher lipophilicity of the esters resulting in higher concentration in the outermost layers, or discrepancies between the experimental and the calculated solubility. The unexpectedly high k_p for the captopril ester might have been explained by a mechanism of self-enhancement (i.e. Al-Saidan 2004). However, a comparison between experimentally measured (Wu et al 1997) and predicted values (Potts & Guy 1992; Moss & Cronin 2002) and particularly the range of data would indicate considerable overlap between both sets of results. Therefore, there was no evidence of self-enhancement in the permeation of captopril or its esters.

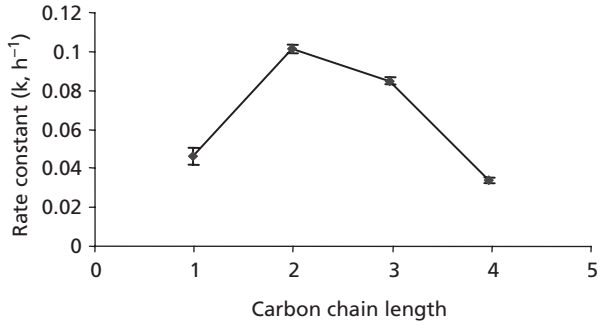

Figure 6 The in-vitro metabolism of captopril carboxyl ester prodrugs (n = 4).

In-vitro metabolism of prodrugs

The results of the in-vitro metabolism of prodrugs is shown in Figure 6. Metabolism appeared to proceed via a pseudo first-order mechanism. Only the C_1–C_4 prodrugs were examined, due to substantial decreases in solubility beyond this point. All the prodrugs reverted rapidly to the parent molecule (captopril). The rate of metabolism indicated that the ethyl and propyl prodrugs were metabolized most rapidly, and that metabolism was slower for the methyl and butyl prodrugs. This was beneficial in terms of prodrug solubility, and also mirrored the increase in flux observed in diffusion experiments for the ethyl and propyl prodrugs, suggesting that metabolic activity might have significantly influenced flux.

The rapid metabolic reversion of prodrugs to captopril is an essential aspect of the proposed mechanism of drug delivery. Nevertheless, it has been demonstrated also that the captopril methyl ester prodrug exerts significant ACE-inhibitory activity despite the loss of the carboxyl functionality (Ingram et al 2004). While such a pharmacological profile is common with other drugs and their metabolites (i.e. verapamil and its main metabolite, norverapamil) it is still important, both clinically and toxicologically, to demonstrate the complete reversion of the prodrugs to captopril and the appropriate alcohol.

Conclusions

QSPRs for percutaneous absorption did not correlate with experimentally determined findings as expected. QSPR models were used in the expectation that prodrugs of captopril could be designed to optimize permeation across skin. Maximal flux values were calculated as the product of k_p and solubility estimates, but did not correlate with experimental results. The predicted changes were observed experimentally only up to a point but failed thereafter – at log P values of greater than 3.0–3.5, the models appeared to fail to predict

percutaneous absorption accurately. This was perhaps to be expected, given the range of molecules in Flynn's original dataset (Flynn 1990). In addition, the decrease in aqueous solubility observed as chain length increase was also of importance, and may have reflected the findings of Magnusson et al (2004). Therefore, QSPRs may be useful guides for maximizing drug delivery, but their use is limited by the physicochemical properties of molecules as well as the expected formulation factors. The use of non-linear modelling may allow a better understanding, and prediction, of percutaneous absorption, particularly for molecules of higher lipophilicities where the QSPR models appeared to depart most from experimental results. Our experimental findings suggested that the ethyl carboxyl ester prodrug was the best candidate for transdermal drug delivery.

References

Al-Saidan, S. M. (2004) Transdermal self-permeation enhancement of ibuprofen. *J. Control. Release* **100**: 199–209

Barry, B. W. (1983) Dermatological formulations, percutaneous absorption. In: *Drugs and the pharmaceutical sciences*. Marcel Dekker Inc., New York, Ch. 18

British Pharmacopoeia (2003) Captopril monograph. Vol. 1, HMSO, London, pp 324–325

Bronaugh, R. L., Maibach, H. I. (1999) *Percutaneous absorption. Drugs – cosmetics – mechanisms – methodology*. Marcel Dekker Inc., London.

Brown, S. L., Rossi, J. E. (1989) A simple method for estimating dermal absorption of chemicals in water. *Chemosphere* **19**: 1989–2001

Collier, S. W., Sheikh, N. M., Sakra, A., Lichtin, J. L., Stewart, R. F., Bronaugh, R. L. (1989) Maintenance of skin viability during in vitro percutaneous absorption/metabolism studies. *Toxicol. Appl. Pharmacol*. **99**: 522–533

Cronin, M. T. D., Dearden, J. C., Gupta, R., Moss, G. P. (1998) An investigation of the mechanism of flux across polydimethylsiloxane membranes by use of quantitative structure-permeability relationships. *J. Pharm. Pharmacol*. **50**: 143–152

Cronin, M. T. D., Dearden, J. C., Moss, G. P., Murray-Dickson, G. (1999) Investigation of the mechanism of flux across human skin in vitro by quantitative structure-permeability relationships. *Eur. J. Pharm. Sci*. **7**: 325–330

Doh, H. J., Cho, W. J., Yong, C. S., Choi, H. G., Kim, J. S., Lee, C. H., Kim, D. D. (2003) Synthesis and evaluation of ketorolac ester prodrugs for transdermal delivery. *J. Pharm. Sci*. **92**: 1008–1017

Fiserova-Bergerova, V., Pierce, J. T., Droz, P. O. (1990) Dermal absorption potential of industrial chemicals, criteria for skin notation. *Am. J. Ind. Med*. **17**: 617–635

Flynn, G. L. (1990) Physicochemical determinants of skin absorption. In: Gerrity, T. R., Henry, C. J. (eds) *Principles of route-to-route extrapolation for risk assessment*. Elsevier, New York. pp 93–127

Fourie, L., Breytenbach, J. C., Du Plessis, J., Goosen, C., Swart, H., Hadgraft, J. (2004) Percutaneous delivery of carbamazepine and selected N-alkyl and N-hydroxyalkyl analogues. *Int. J. Pharm*. **279**: 59–66

Geinoz, S., Rey, S., Boss, G., Bunge, A. L., Guy, R. H., Carrupt, P. A., Reist, M., Testa, B. (2002) Quantitative structure-permeation relationships for solute transport across silicone membranes. *Pharm. Res*. **19**: 1622–1629

Geinoz, S., Guy, R. H., Testa, B., Carrupt, P. A. (2004) Quantitative structure-permeation relationships (QSPeRs) to predict skin permeation: a critical evaluation. *Pharm. Res*. **21**: 83–92

Guy, R. H., Potts, R. O. (1992) Structure-permeability relationships in percutaneous penetration. *J. Pharm. Sci*. **81**: 603–604

Ingram, M. J., Gard, P. R., Patel, N., Moss, G. P., Gullick, D. R. (2004) ACE-inhibitory activity of captopril methyl ester prodrug. *J. Pharm. Pharmacol*. **56** (Suppl.): S88

Kalia, Y. N., Naik, A., Garrison, J., Guy, R. H. (2004) Iontophoretic drug delivery. *Adv. Drug Del. Rev*. **56**: 619–658

Lebosse, R., Ducruet, V., Feigenbaum, A. (1996) Aqueous solubility determination of volatile organic compounds by capillary gas chromatography. *J. High Res. Chromat*. **19**: 413–416

Leboulanger, B., Guy, R. H., Delgado-Charro, M. B. (2004) Reverse iontophoresis for non-invasive transdermal monitoring. *Physiol. Meas*. **25**: R35–R50

Lopez, A., Faus, V., Diez-Sales, O., Herraez, M. (1998) Skin permeation model of phenyl alcohols, comparison of experimental conditions. *Int. J. Pharm*. **173**: 183–191

Magnusson, B. M., Anissimov, Y. G., Cross, S. E., Roberts, M. S. (2004) Molecular size as the main determinant of solute maximum flux across skin. *J. Invest. Dermatol*. **122**: 993–999

Martinez, J. C., Fuentes, M. J., Armentia, A., Vega, J. M., Fernandez, A. (2001) Dermatitis to captopril. *Allergol Immunopathol. (Madr.)* **29**: 279–280

McKone, T. E., Howd, R. A. (1992) Estimating dermal uptake of non-ionic organic chemicals from water and soil, I Unified fugacity-based models for risk assessment. *Risk Anal*. **12**: 543–557

Moss, G. P., Cronin, M. T. D. (2002) Quantitative structure-permeability relationships for percutaneous absorption, re-analysis of steroid data. *Int. J. Pharm*. **238**: 105–109

Moss, G. P., Dearden, J. C., Patel, H., Cronin, M. T. D. (2002) Quantitative structure-permeability relationships (QSPRs) for percutaneous absorption. *Toxicol. In Vitro* **16**: 299–317

Ostacolo, C., Marra, F., Laneri, S., Sacchi, A., Nicoli, C., Padula, C., Santi, P. (2004) α-Tocopherol pro-vitamins, synthesis, hydrolysis and accumulation in rabbit ear skin. *J. Control. Release* **99**: 403–413

Patel, H., ten Berge, W., Cronin, M. T. D. (2002) Quantitative structure-activity relationships (QSARs) for the prediction of skin permeation of exogenous chemicals. *Chemosphere* **48**: 603–613

Potts, R. O., Guy, R. H. (1992) Predicting skin permeability. *Pharm. Res*. **9**: 663–669

Potts, R. O., Guy, R. H. (1995) A predictive algorithm for skin permeability, the effects of molecular size and hydrogen bond activity. *Pharm. Res*. **12**: 1628–1633

Ranadive, S. A., Chen, A. X., Serajuddin, A. T. M. (1992) Relative lipophilicities and structural pharmacological considerations of various angiotensin-converting enzyme ACE inhibitors. *Pharm. Res*. **9**: 1480–1486

Robinson, P. J. (1993) *A composite model for predicting dermal penetration in vivo.* Human and Environmental Safety Division, The Proctor & Gamble Company, OH, USA. Personal communication

Stinchcomb, A. L., Swaan, P. W., Ekabo, O., Harris, K. K., Browe, J., Hammell, D. C., Cooperman, T. A., Pearsall, M. (2002) Straight-chain naltrexone ester prodrugs, diffusion and concurrent esterase biotransformation in human skin. *J. Pharm. Sci*. **91** 2571–2578

Tai, D. F., Chao, Y. H., Huang, C. Y., Luo, J. M., Lin, Y. T., Wu, S. H. (1995) Resolution of ibuprofen catalysed with free and immobilized lipases. *J. Chin. Chem. Soc*. **42**: 801–807

Taylor, L. J., Lee, R. S., Long, M., Rawlings, A. V., Tubek, J., Whitehead, L., Moss, G. P. (2002) Effect of occlusion on the percutaneous penetration of linoleic acid and glycerol. *Int. J. Pharm*. **249**: 157–164

Udata, C., Tirucherai, G., Mitra, A. K. (1999) Synthesis, stereoselective enzymatic hydrolysis, and skin permeation of diastereomeric propranolol ester prodrugs. *J. Pharm. Sci*. **88**: 544–550

Valenta, C., Auner, B. G. (2004) The use of polymers for dermal and transdermal delivery. *Eur. J. Pharm. Biopharm*. **58**: 279–289

Wester, R. C., Noonan, P. K. (1980) Relevance of animal models for percutaneous absorption. *Int. J. Pharm*. **7**: 99–110

Wilschut, A., Tenberge, W. F., Robinson, P. J., McKone, T. E. (1995) Estimating skin permeation. The validation of five mathematical skin permeation models. *Chemosphere* **30**: 1275–1296

Woolfson, A. D., McCafferty, D. F., McGowan, K. (1992) Percutaneous penetration characteristics of amethocaine through porcine and human skin. *Int. J. Pharm*. **78**: 209–216

Woolfson, A. D., McCafferty, D. F., Moss, G. P. (1998) Development and characterisation of a moisture-activated bioadhesive drug delivery system for percutaneous local anaesthesia. *Int. J. Pharm*. **169**: 83–94

Wu, P.-C., Huang, Y.-B., Fang, J.-Y., Tsai, Y.-H. (1997) In vitro percutaneouus absorption of captopril. *Int. J. Pharm*. **48**: 41–46